Proceedings of
2002 ASME International Mechanical Engineering Congress and Exposition
November 17-22, 2002, New Orleans, LA

IMECE2002/HTD- 34246

MODELING OF FORCED CONVECTION IN AN ELECTRONIC DEVICE HEAT SINK AS POROUS MEDIA FLOW

Andrej Horvat
Institute "Jožef Stefan"
Reactor Engineering Division
Jamova 39, SI-1111 Ljubljana, Slovenia

Ivan Catton
Morrin-Martinelli-Gier Memorial Heat Transfer Laboratory
Department of Mechanical and Aerospace Engineering
University of California, Los Angeles

ABSTRACT

An algorithm for simulation of conjugate heat transfer used to find the most suitable geometry for an electronic chip heat sink is described. Applying Volume Averaging Theory (VAT) to a system of transport equations, a heat exchanger structure was modeled as a homogeneous porous media. The interaction between the fluid and the structure, the VAT equation closure requirement, was accomplished with drag and heat transfer coefficients, which were taken from the available literature and inserted into a computer code. The example calculations were performed for an aluminum heat sink exposed to force convection airflow. The geometry of the simulation domain and boundary conditions followed the geometry of the experimental test section. The comparison of the whole-section drag coefficient and Nusselt number as functions of Reynolds number shows a good agreement with the experimental data. The calculated temperature fields reveal the local heat flow distribution and enable further improvements of the heat sink geometry.

NOMENCLATURE

A	area	***Subscripts/Superscripts***	
C_d	drag coefficient	*b*	base
d	diameter	*f*	fluid
h	heat transfer coeff.	*g*	ground
H	domain height	*h*	hydraulic
L	domain length	*in*	inflow
m	mass flow rate	*o*	interfacial area
Nu	Nusselt number	*out*	outflow
p	pressure, pitch	*s*	solid
Q	heat flow rate	*x,y,z*	spatial directions
Re	Reynolds number		
S	specific interfacial area	***Greek letters***	
T	temperature	α	void fraction
u	velocity	ρ	density
V	volume	λ	hermal conductivity
W	domain width	μ	ynamic viscosity
x,y,z	spatial coordinates	ν	inematic viscosity
		Ω	olume

INTRODUCTION

Heat exchangers can be found in a number of different industrial sectors where a need to transport heat from media to media exist. Consequently, wide spread heat exchanger application has caused development to take place in a piecemeal fashion in a number of rather unrelated areas. Much detailed technology, familiar in one sector, progressed only slowly over the boundary into another sector [1].

To overcome historic difficulties, the unified description for heat and fluid flow has to be found. For this purpose, we chose Volume Averaging Theory (VAT) presented by Whiteker [2] and further developed by Travkin and Catton [3 & 4] as one of suitable options. Namely, applying VAT to a system of equations, transport processes in a heat exchanger can be modeled as a homogeneous porous media flow. The VAT system of equations, however, require additional modeling or experimental values to describe the interaction between fluid and heat sink structure.

In the present paper VAT was used to model heat transfer process in a computer chip heat sink (Fig. 1). The geometry and boundary conditions closely follow the experimental studies at the Morrin-Martinelli-Gier Memorial Heat Transfer Laboratory at University of California, Los Angeles.

The finite volume calculations were performed for an aluminum heat sink with a staggered pin-fin arrangement. Three sets of calculations were made, each with different thermal input. In all cases, the pitch-to-diameter ratio in the streamwise

direction was set to p_x/d = 1.06 and in transverse direction to p_y/d = 2.12. The Reynolds number, based on hydraulic diameter, spanned from Re_h = 159 to Re_h = 1898.

The results will show three-dimensional temperature field in the fluid flow as well as in the heat sink structure for a thermal input of 125W. Furthermore, the comparison of a whole-section drag coefficient C_d and Nusselt number Nu will demonstrate an excellent agreement with the available experimental data [5].

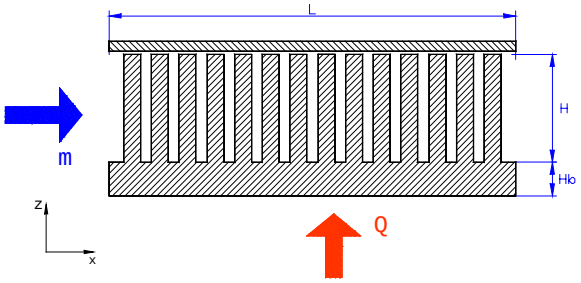

Figure 1: Experimental test section.

MODEL APPROACH

The airflow through an aluminum chip cooler structure can be described with basic mass, momentum and heat transport equations:

$$\partial_i u_i = 0 \tag{1}$$

$$\rho_f u_j \partial_j u_i = -\partial_i p_f + \mu_f \partial_j \partial_j u_i \tag{2}$$

$$\rho_f c_f u_j \partial_j T_f = \lambda_f \partial_j \partial_j T_f \tag{3}$$

In the solid phase, heat is transferred only by thermal conduction:

$$0 = \lambda_s \partial_j \partial_j T_s \tag{4}$$

In order to develop a unified approach for heat exchanger calculations, the transport equations (1-4) are averaged over a periodic control volume (see [4] for details). Thus, the fluid phase transport equations are transformed to

$$\partial_i \hat{u}_i = 0 \tag{5}$$

$$\alpha_f \rho_f \hat{u}_j \partial_j \hat{u}_i V = -\alpha_f \Delta \hat{p}_f A + \alpha_f \mu_f \partial_j \partial_j \hat{u}_i V - \frac{1}{A}\int_{\partial A} (p_f + \mu_f \partial_j \hat{u}_i) d\vec{\Omega} \tag{6}$$

$$\alpha_f \rho_f c_f \hat{u}_j \partial_j \hat{T}_f V = \alpha_f \lambda_f \partial_j \partial_j \hat{T}_f V + \frac{1}{A}\int_{\partial A} \lambda_f \partial_j T_f d\vec{\Omega} \tag{7}$$

Similarly, the solid phase transport equation is written in averaged form as

$$0 = \alpha_s \lambda_s \partial_j \partial_j \hat{T}_s V + \frac{1}{A}\int_{\partial \Omega} \lambda_s \partial_j T_s d\vec{\Omega} \tag{8}$$

To predict the temperature in the heat exchanger solid base, a separate energy transport equation has to be written

$$0 = \lambda_s \partial_j \partial_j \hat{T}_b V \tag{9}$$

As a result of the volumetric averaging, the spatial scale of the phase-averaged values (eqs. 5-9) is much larger than the scale of the local values (eqs. 1-4). The integrals in eqs. (6-8) capture momentum and energy transport on the fluid-solid interface. Similar to turbulent flow, separate models in the form of closure relations are needed. In the present case, the integrals in eqs. (6-8) are replaced with drag relation

$$\alpha_f \rho_f \hat{u}_j \partial_j \hat{u}_i V = -\alpha_f \Delta \hat{p}_f A + \alpha_f \mu_f \partial_j \partial_j \hat{u}_i V - \frac{1}{2} C_d \rho_f \hat{u}_i^2 A_o \tag{10}$$

and heat transfer relation

$$\alpha_f \rho_f c_f \hat{u}_j \partial_j \hat{T}_f V = \alpha_f \lambda_f \partial_j \partial_j \hat{T}_f V - h\left(\hat{T}_f - \hat{T}_s\right) A_o \tag{11}$$

$$0 = \alpha_s \lambda_s \partial_j \partial_j \hat{T}_s + h\left(\hat{T}_f - \hat{T}_s\right) A_o \tag{12}$$

To further simplify the simulated system, the fluid flow was taken to be unidirectional with a constant pressure drop. As a consequence, the velocity changes only transverse to the flow direction. This means that the streamwise pressure gradient across the entire simulation domain is balanced with shear stresses in the transverse (y and z) directions:

$$-\alpha_f \mu_f \left(\partial_y \partial_y \hat{u}_x + \partial_z \partial_z \hat{u}_x\right) + \frac{1}{2} C_d \rho_f \hat{u}^2 S = \frac{\Delta \hat{p}}{L} \tag{13}$$

where Δp is positive.

As shown by the energy eq. (11), thermal convection in the fluid phase is balanced with diffusion due to temperature gradients as well as with heat transferred from conducting pin-fins:

$$\alpha_f \rho_f c_f \hat{u}_x \partial_x \hat{T}_f = \alpha_f \lambda_f \left(\partial_x \partial_x \hat{T}_f + \partial_y \partial_y \hat{T}_f + \partial_z \partial_z \hat{T}_f\right) - h\left(\hat{T}_f - \hat{T}_s\right) S \tag{14}$$

The chip cooler structure in each control volume is only loosely connected in the horizontal directions. As a consequence, only the thermal diffusion in the vertical direction is in balance with heat leaving the structure through a fluid-solid interface, whereas the thermal diffusion in the horizontal

directions can be neglected. This simplifies the energy equation for the solid phase to:

$$0=\alpha_s\lambda_s\partial_z\partial_z\hat{T}_s+h\left(\hat{T}_f-\hat{T}_s\right)S \tag{15}$$

For heat transfer in the solid base the diffusion equation has to be written for all three dimensions:

$$0=\lambda_s\left(\partial_x\partial_x\hat{T}_b+\partial_y\partial_y\hat{T}_b+\partial_z\partial_z\hat{T}_b\right) \tag{16}$$

The Volume Averaging Technique (VAT) leads to a closure problem, where interface exchange of momentum and heat between fluid and solid phase have to be described with additional empirical relations for the local drag coefficient C_d (eq. 13) and the local heat transfer coefficient h (eqs. 14 & 15). For these coefficients, reliable experimental data were found in [8-10].

The resulting model of homogenous porous media flow, summarized in eqs. (13-16), significantly differs from Darcy's, Forchheimer's or Brinkman's models. The reason is not in different physics, but rather in the mathematical consistency of the developed transport eqs. (5-9) and availability of empirical values for the drag coefficient C_d and the heat transfer coefficient h.

SIMULATION DOMAIN

The geometry of the simulation domain as well as the boundary conditions for eqs. (13-16) follows the geometry of the experimental test section [5]

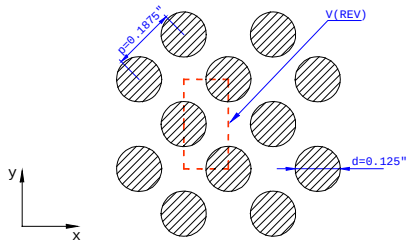

Figure 2: Pin-fins arrangement in the simulated case.

The general arrangement of pin-fins in the simulation domain is given in Fig. 2. The diameter of pin-fins was d = 0.003175m (0.125"). The pitch-to-diameter ratio in streamwise direction was set to p_x/d = 1.06 and in transverse direction to p_y/d = 2.12. The simulation domain consisted of 34 rows of pin-fins in the streamwise direction and 17 rows of pin-fins in the transverse direction.

The no-slip boundary conditions for the momentum eq. (13) were implemented for all 4 walls parallel with the flow direction:

$$\hat{u}_x(0,z)=0\,,\quad \hat{u}_x(W,z)=0\,,\quad \hat{u}_x(y,0)=0\,,\ \hat{u}_x(y,H)=0 \tag{17}$$

As a flow driving force, the whole-section pressure drop Δp was prescribed. The absolute values are summarized in Table 1.

For the fluid-phase energy equation (14), the simulation domain inflow and the bottom wall were taken as isothermal:

$$\hat{T}_f(0,y,z)=T_{in}\,,\quad \hat{T}_f(x,y,0)=T_{if} \tag{18}$$

whereas the other walls were considered as adiabatic:

$$\begin{aligned}&\partial_x\hat{T}_f(L,y,z)=0\,,\ \partial_y\hat{T}_f(x,0,z)=0\,,\\&\partial_y\hat{T}_f(x,W,z)=0\,,\ \partial_z\hat{T}_f(x,y,H)=0\end{aligned} \tag{19}$$

For the solid-phase energy equation (15), the bottom wall was prescribed as isothermal, whereas the top wall was assumed to be adiabatic:

$$\hat{T}_s(x,y,0)=T_{if}\,,\quad \partial_z\hat{T}_s(x,y,H)=0 \tag{20}$$

The boundary conditions for the solid base show the coupled nature of heat transfer between the homogenous porous media flow (eqs. 14 & 15) and the base (eq. 16). Namely, the heat fluxes on the interface has to be equal:

$$\lambda_s\partial_z\hat{T}_b(x,y,0)=\alpha_f\lambda_f\partial_z\hat{T}_f(x,y,0)+\alpha_s\lambda_s\partial_z\hat{T}_s(x,y,0) \tag{21}$$

On the base bottom the isothermal boundary conditions were prescribed

$$\hat{T}_b(x,y,-H_b)=T_g \tag{22}$$

whereas the vertical walls were taken as adiabatic

$$\begin{aligned}&\partial_x\hat{T}_b(0,y,z)=0\,,\ \partial_x\hat{T}_b(L,y,z)=0\,,\\&\partial_y\hat{T}_b(x,0,z)=0\,,\ \partial_y\hat{T}_b(x,W,z)=0\end{aligned} \tag{23}$$

Although, the calculations were made for thermal power of 50, 125 and 220W, the present paper shows the results for 125W only. For this case the preset pressure drops and absolute temperatures in different simulation cases are summarized in Table 1.

Table 1: Boundary conditions - preset values.

No.	Δp [Pa]	T_{in} [°C]	T_g [°C]	No.	Δp [Pa]	T_{in} [°C]	T_g [°C]
1	5.0	23.0	103.8	**5**	74.7	23.2	41.8
2	10.0	23.0	74.6	**6**	179.3	23.2	35.7
3	20.0	23.0	58.8	**7**	274.0	23.0	33.6
4	40.0	23.0	48.2	**8**	361.1	22.8	32.3

NUMERICAL METHODS

The transport eqs. (13-16) and boundary equations (17-23) were transformed into dimensionless form and then discretized following principles of the finite volume methods [6 & 7]. Due to the boundary conditions (17-23), the velocity in the streamwise direction u_x as well as the solid-phase temperature T_s were described as two-dimensional scalar fields, whereas the fluid-phase temperature T_f and the base temperature T_b as a three-dimensional scalar field. This resulted in a non-symmetric five diagonal matrix system for two-dimensional scalar fields and a seven diagonal matrix system for three-dimensional scalar fields.

In order to invert the matrix systems efficiently, a preconditioned conjugate gradient method, described in [11], was adopted for this specific problem.

RESULTS AND DISCUSSION

The calculations were performed for imposed pressure drops, which are summarized in Table 1. They cause a fluid flow with Reynolds numbers from Re_h = 159 to 1898, where the definition of the Reynolds number is based on the hydraulic diameter d_h of the hypothetical porous media channel

$$Re_h = \frac{\bar{\bar{u}}_x}{\nu_f} d_h = \frac{\bar{\bar{u}}_x}{\nu_f}\left(4\frac{\Omega_f}{S}\right) \tag{24}$$

In all cases the thermal flow from the isothermal bottom was adjusted to 125 W to match the experimental setup [5].

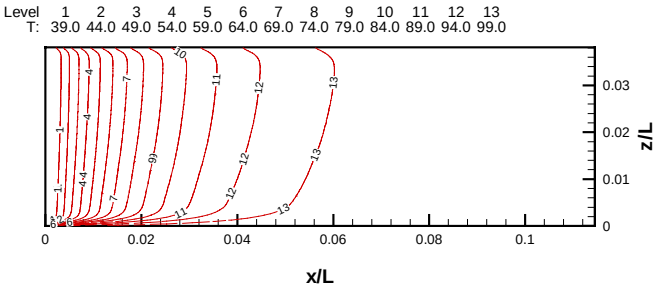

Figure 3: Temperature field in fluid phase, Q = 125W, Re_h = 159.

The cross-section of the temperature fields for the example calculations are presented in Figs. 3-6 where the temperature is marked with isotherms. Figs. 3 shows temperature field in the fluid-phase and Fig. 4 in the solid-phase and the base at Reynolds number Re_h=159.

It can be seen in Fig. 3 that the temperature field in the fluid-phase is poorly developed. The isotherms are almost vertical, which means that the base does not have significant influence on temperature field development; most of the heat is transferred from the pin-fins to the flow. The situation is changes toward outflow on the right. The conducting pin-fins immersed into a cross-flow manage to heat the fluid almost to the solid phase temperature after passing a half the test section.

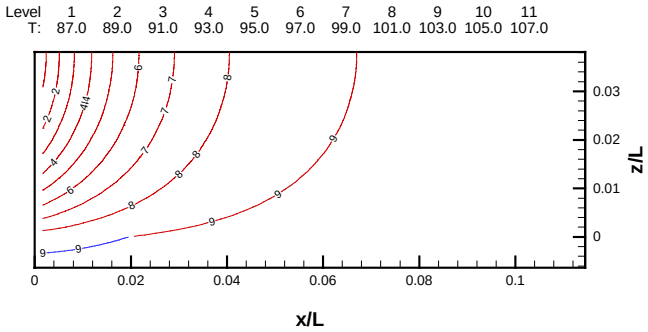

Figure 4: Temperature field in solid phase, Q = 125W, Re_h = 159.

Fig. 4 shows that the solid-phase temperature is the lowest close to the upper left edge of the simulation domain due to cold air inflow and a large distance from the heated bottom. As it is seen, the temperature rises fast from the inflow on the left, leaving the right half of the heat sink structure isothermal.

In the next case (Figs. 5 & 6) the Reynolds number Re_h is increased to 1898. The fluid-phase temperature field in Fig. 5 is much more developed as in the previous case. Close to inflow the isotherms are vertical and the fluid phase is heated rapidly across whole height of the test section.

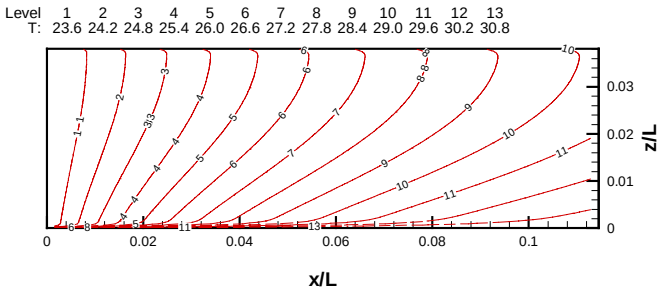

Figure 5: Temperature field in fluid phase, Q = 125W, Re_h = 1898.

Further downstream, as the fluid is heated, the isotherms become tilted due to decreased rate of heat passing from the structure to the fluid-phase. In addition, the increased influence of thermal input through the bottom results in gradual horizontal thermal stratification of passing air. With increasing thermal power or/and length of the simulation domain, the horizontal stratification becomes stronger.

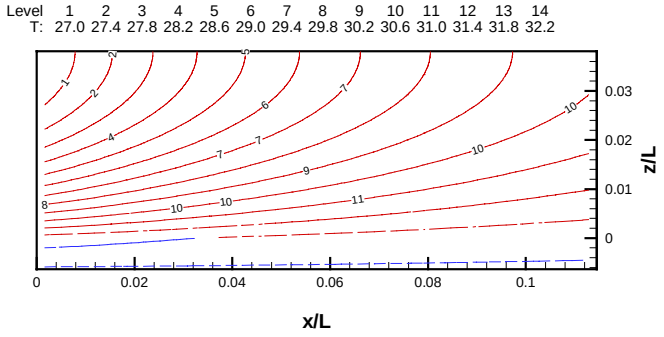

Figure 6: Temperature field in solid phase, Q = 125W, Re_h = 1898.

Fig. 6 presents the temperature field in the solid structure and the base of the heat sink. Again the horizontal stratification is much more feasible as in the case of Reynolds number Re_h = 159. The spacing between isotherms in the base ($z < 0$) is larger than in the solid structure ($z > 0$), which indicates that temperature gradients in the heat sink base are smaller than in the solid structure. From on these observations, we can conclude that, due to force convection, the effective conductivity of the heat sink is much larger than thermal conductivity of solid-phase (aluminum) alone.

More general comparisons of the whole-section drag coefficient C_d ,

$$\overline{C}_d = \frac{2\Delta\hat{p}}{\rho_f (\bar{\hat{u}}_x)^2 LS} \tag{25}$$

and Nusselt number Nu

$$\overline{Nu} = \frac{\dot{\hat{Q}} d_h}{(\hat{T}_b - \hat{T}_{in}) A_g \lambda_f} \tag{26}$$

were also made. The results from the finite volume method calculations were compared with experimental data [5].

The comparison in Fig. 7 shows the whole-section drag coefficient C_d (eq. 25) as a function of the Reynolds number Re_h (eq. 24). It reveals an excellent agreement with the experimental data. Also the comparison of the Nusselt number distributions in Fig. 8 shows that only the slight difference to the experimental data appears at higher Reynolds number. Possible reason for this difference can be found in increasing turbulence, which was not taken into account in both computational models.

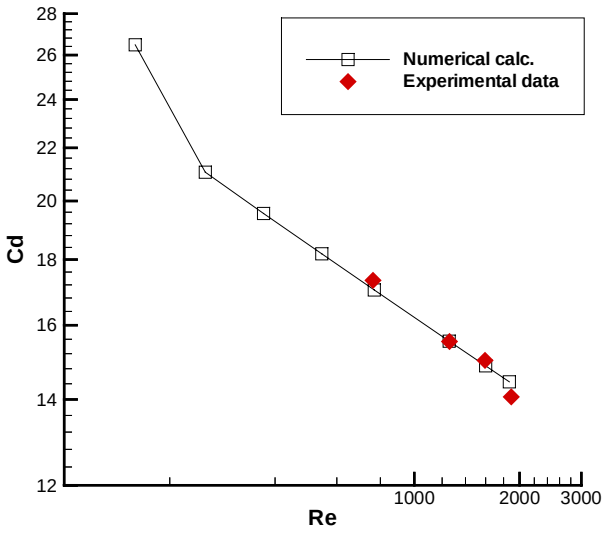

Figure 7: Reynolds number Re_h dependence of drag factor C_d , 125W of thermal power.

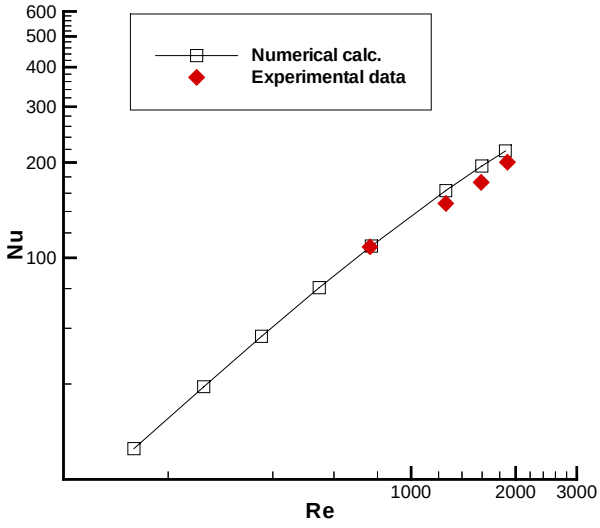

Figure 8: Reynolds number Re_h dependence of Nusselt number Nu , 125W of thermal power.

CONCLUSIONS

The present paper describes an effort to develop a fast running numerical algorithm for calculation of conjugate heat transfer through a heat sink with a generalized geometry. For that purpose the Volume Averaging Technique (VAT) was employed in order to model the heat sink structure as the homogeneous porous media.

The example calculations were made for an aluminum heat sink with staggered pin-fins arrangement cooled with airflow. The geometry of the simulation domain and boundary

conditions followed the geometry of the experimental test section used in the Morrin-Martinelli-Gier Memorial Heat Transfer Laboratory at University of California, Los Angeles. The local values of drag and heat transfer coefficients that were needed to close the transport equations were taken from [8-10]. The resulting partial differential equations were discretized using the momentum and energy conservation properties of the finite volume method. The resulting system of semilinear equations was solved with a preconditioned conjugate gradient method.

To test the calculation procedure, a comparison with the experimental data [5] was made. The calculated values of the whole-section drag coefficient and the Nusselt number show an excellent agreement with already published data. Plotted three-dimensional temperature fields reveal the local heat transfer conditions and enable corrections and optimization of the heat exchanger geometry.

The present results demonstrate that the selected approach is appropriate for heat exchanger calculations where a thermal conductivity of a solid-phase has to be taken into account. The example calculations also verify that the developed numerical code yields sufficiently accurate results to be applicable also elsewhere.

ACKNOWLEDGEMENTS

The first author's financial support by the Kerze-Cheyovich Research Assistantship, the DARPA Heretic Program and Ministry of Education, Science and Sport of Republic Slovenia is gratefully acknowledged.

REFERENCES

[1] Hesselgreaves, J.E., *Compact Heat Exchangers Selection, Design and Operation*, Pergamon Press, 2001.

[2] Whitaker, S., Diffusion and Dispersion in Porous Media, *AIChE Journal*, Vol. 13, No. 3, pp. 420-427, 1967.

[3] Travkin, V., Catton, I., A Two Temperature Model for Fluid Flow and Heat Transfer in a Porous Layer, *J. Fluid Engineering*, Vol. 117, pp. 181-188, 1995.

[4] Travkin, V., Catton, I., Transport Phenomena in Heterogeneous Media Based on Volume Averaging Theory, *Advans. Heat Trasfer*, Vol. 34, pp. 1-143, 1999.

[5] Rizzi, M., Canino, M., Hu, K., Jones, S., Travkin, V., Catton, I., Experimental Investigation of Pin Fin Heat Sink Effectiveness, *Proc. of the 35th National Heat Transfer Conference*, Anaheim, California, 2001.

[6] Horvat, A., Rizzi, M., Catton, I., *Advances in Computational Methods In Heat Transfer IX* : *Numerical Investigation of Chip Cooling Using Volume Averaging Technique* (*VAT*), Computational Mechanics Publications, Southampton, UK, 2002.

[7] Versteeg, H.K., Malalasekera, W., *An Introduction to Computational Fluid Dynamics, The Finite Volume Method*, Longman Scientific & Technical: England, pp. 103-133, 1995.

[8] Launder, B.E., Massey, T.H., The Numerical Prediction of Viscous Flow and Heat Transfer in Tube Bank. *Trans. ASME J. Heat Transfer*, Vol. 100, pp. 565-571, 1978.

[9] Kays, W. M., London, A. L., *Compact Heat Exchangers*. 3rd Ed. Krieger Publishing Company, Malabar, Florida, pp. 146-147, 1998.

[10] Žukauskas, A.A., Ulinskas, R., Efficiency Parameters for Heat Transfer in Tube Banks. *J. Heat Transfer Engineering*, Vol.5, No.1, pp. 19-25, 1985.

[11] Ferziger, J.H., Perić, M., *Computational Method for Fluid Mechanics, Chapter 5: Solution of Linear Equation Systems*. Springer Verlag, Berlin, pp. 85-127, 1996.